International Journal of Computer Assisted Radiology and Surgery (2020) 15:725–735
https://doi.org/10.1007/s11548-020-02124-z

ORIGINAL ARTICLE

Virtual septoplasty: a method to predict surgical outcomes for patients with nasal airway obstruction

Masoud Gh. Moghaddam[1,2] · Guilherme J. M. Garcia[1,2] · Dennis O. Frank-Ito[3,4,5] · Julia S. Kimbell[6] · John S. Rhee[1]

Received: 21 August 2019 / Accepted: 10 February 2020 / Published online: 20 February 2020

Abstract

Purpose A deviated nasal septum is the most common etiology for nasal airway obstruction (NAO), and septoplasty is the most common surgical procedure performed by ear–nose–throat surgeons in adults. However, quantitative criteria are rarely adopted to select patients for surgery, which may explain why up to 50% of patients report persistent or recurrent symptoms of nasal obstruction postoperatively. This study reports a systematic virtual surgery method to identify patients who may benefit from septoplasty.

Methods One patient with symptoms of NAO due to a septal deviation was selected to illustrate the virtual surgery concept. Virtual septoplasty was implemented in three steps: (1) determining if septal geometry is abnormal preoperatively, (2) virtually correcting the deviation while preserving the anatomical shape of the septum, and (3) estimating the post-surgical improvement in airflow using computational fluid dynamics. Anatomical and functional changes predicted by the virtual surgery method were compared to a standard septoplasty performed independently from the computational analysis.

Results A benchmark healthy nasal septum geometry was obtained by averaging the septum dimensions of 47 healthy individuals. A comparison of the nasal septum geometry in the NAO patient with the benchmark geometry identified the precise locations where septal deviation and thickness exceeded the healthy range. Good agreement was found between the virtual surgery predictions and the actual surgical outcomes for both airspace minimal cross-sectional area (0.05 cm^2 pre-surgery, 0.54 cm^2 virtual surgery, 0.50 cm^2 actual surgery) and nasal resistance (0.91 Pa.s/ml pre-surgery, 0.08 Pa.s/ml virtual surgery, 0.08 Pa.s/ml actual surgery).

Conclusions Previous virtual surgery methods for NAO were based on manual edits and subjective criteria. The virtual septoplasty method proposed in this study is objective and has the potential to be fully automated. Future implementation of this method in virtual surgery planning software has the potential to improve septoplasty outcomes.

Keywords Virtual surgery planning · Nasal airway obstruction due to a deviated septum · Computational fluid dynamics (CFD) simulations of nasal airflow · Nasal resistance · Healthy subjects

Masoud Gh. Moghaddam and Guilherme J. M. Garcia have contributed equally to this paper.

✉ Guilherme J. M. Garcia
ggarcia@mcw.edu

[1] Department of Otolaryngology and Communication Sciences, Medical College of Wisconsin, Milwaukee, WI, USA

[2] Joint Department of Biomedical Engineering, Marquette University and The Medical College of Wisconsin, Milwaukee, WI, USA

[3] Department of Head and Neck Surgery and Communication Sciences, Duke University Medical Center, Durham, NC, USA

[4] Computational Biology and Bioinformatics Program, Duke University, Durham, NC, USA

[5] Department of Mechanical Engineering and Materials Science, Duke University, Durham, NC, USA

[6] Department of Otolaryngology/Head and Neck Surgery, University of North Carolina School of Medicine, Chapel Hill, NC, USA

Introduction

Virtual surgery planning is emerging as a technology to assist ear–nose–throat surgeons in surgical planning for patients with nasal airway obstruction (NAO) [1–4]. Currently, surgical planning for NAO is based on patients' subjective sensation of obstruction, physical examination findings, and surgeon judgment (which is prone to bias) without any objective measurement of nasal airflow. There is hope that virtual surgery planning based on computational fluid dynamics (CFD) simulations of nasal airflow will help improve the efficacy of NAO surgery, which currently fails to eliminate symptoms in up to 50% of patients in long-term studies [5, 6].

The most common etiology for nasal obstruction is a deviated nasal septum—i.e., a septum that is off midline and/or abnormally shaped (Fig. 1). In 2010, 340,000 patients underwent septoplasty (i.e., surgical correction of the deviated septum) in the United States [7]. In addition to septal deviations, other common causes of NAO are inferior turbinate hypertrophy and nasal valve insufficiency; thus, septoplasty is often performed in conjunction with turbinate surgery and/or functional rhinoplasty.

Septal deviations are very common; about 20–26% of healthy individuals have a deviated nasal septum [8, 9]. Thus, septal deviations are commonly observed during physical examinations and surgeons face the challenging question of determining if a septal deviation causes nasal obstruction in a given patient [10]. Currently, no quantitative criteria to select patients for surgery have been adopted universally. Thresholds have been proposed to identify surgical candidates based on the airspace minimal cross-sectional area measured with acoustic rhinometry or nasal resistance measured with rhinomanometry [11], but these criteria have not been universally adopted due to the poor correlation between acoustic rhinometry, rhinomanometry, and subjective sensation of nasal airflow [12].

This study reports the first systematic virtual surgery method to identify patients who may benefit from septoplasty and to predict post-surgical changes in nasal airflow using CFD. Patients who are good candidates for septoplasty are identified based on two criteria. First, CFD simulations in the pre-surgery nasal anatomy must demonstrate that nasal airflow variables are outside the healthy range [13]. Second, the geometry of the nasal septum must be outside the range of septal shapes observed in healthy individuals. Once a patient is deemed a candidate for surgery, virtual septoplasty is performed in two steps, namely (1) repositioning the septum to its normal midline position and (2) restoring the septum to normal anatomical shape and thickness. This virtual septoplasty method is illustrated by applying it to a patient with a severe septal deviation and highly asymmetric airflow partitioning between the left and right nostrils. The septal geometry and airflow variables in the virtual surgery model are compared to a real septoplasty, which was performed in the same patient independently from the computational modeling. Our results illustrate the potential of virtual surgery planning to predict surgical outcomes in NAO patients.

Materials and methods

Study design

An overview of the virtual septoplasty method is depicted in Fig. 2. First, the geometry of the pre-surgery NAO septum is compared to the benchmark healthy septum geometry obtained from 47 healthy individuals (Section "Benchmark healthy septum geometry"). Second, a virtual septoplasty method that preserves the anatomical shape of the septum and corrects the septal deviation and septal thickness is implemented (Section "Virtual septoplasty method"). Finally, post-surgical changes in nasal airflow are quantified via CFD (Section "Computational fluid dynamics simulations"). This virtual septoplasty method was validated by comparing the predicted changes in septal geometry and nasal airflow with actual changes in a patient who underwent a standard septoplasty.

Cohort demographics

This study was approved by the IRB committees at the Medical College of Wisconsin and Marquette University with informed consent obtained from each patient. A cohort of 47 healthy adults and one NAO patient with septal deviation toward the right cavity was selected (Fig. 1). The patient was a 27-year-old female with preoperative Nasal Obstruction Symptom Evaluation (NOSE) score of 75 in a 100-point scale [14]. She had undergone septoplasty without turbinate reduction and reported symptom improvement (postoperative NOSE score = 10). Both pre-surgery and post-surgery computed tomography (CT) scans were available from a previous study [15, 16, 18]. The virtual septoplasty method was developed independently and blinded from the actual surgery.

The healthy cohort included 19 males and 28 females with a mean age of 48 ± 18 years (range: 18–81 years, median: 52 years). These healthy adults were recruited from a dental clinic and were deemed to have normal subjective scores of nasal patency (NOSE score < 32) and a normal nasal anatomy based on history and CT findings [13]. Patients with a history of nasal surgery, severe nasal trauma resulting in a crooked nose, autoimmune disease, chronic sinusitis, severe allergies, or other sinonasal disease were excluded.

It is important to note that the presence of a septal deviation was not an exclusion criterion in the healthy cohort. Studies of cranial computed tomography scans reveal that 20–26% of

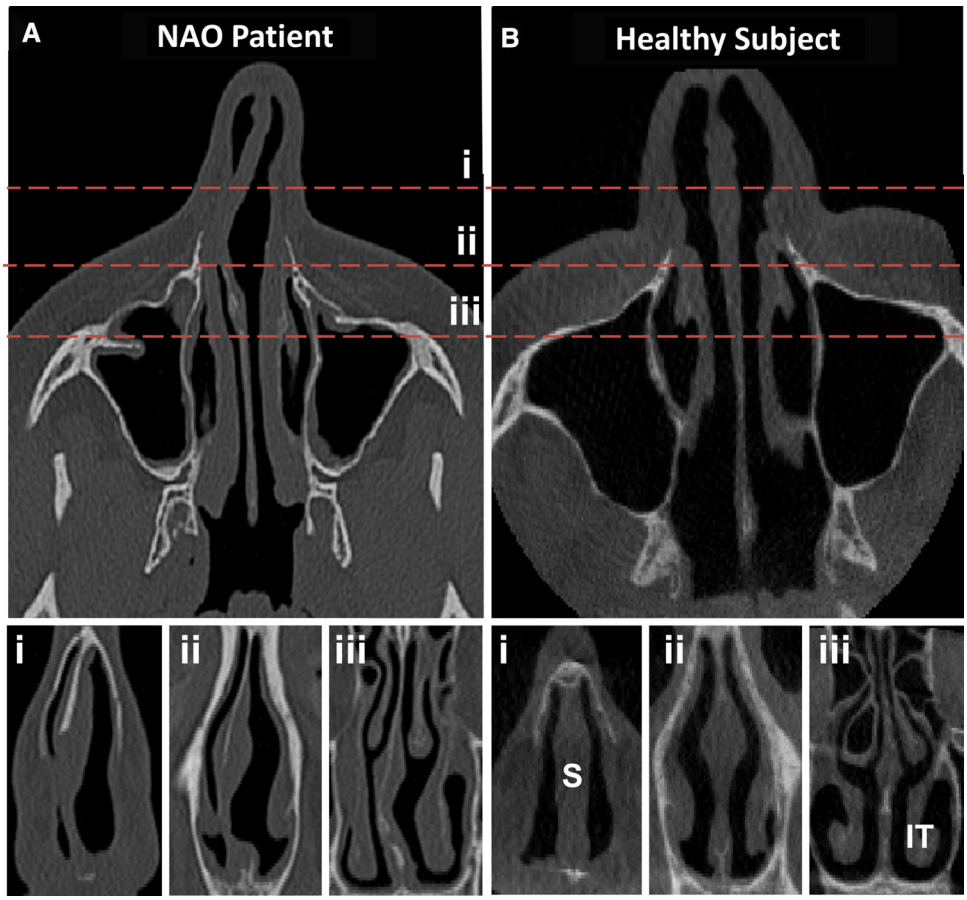

Fig. 1 Computed tomography scans of the nasal cavity in **a** one patient with nasal airway obstruction (NAO) associated with a rightward septal deviation and **b** one healthy subject. The dashed lines in the axial section mark the locations of the coronal sections i, ii, and iii. *S* septum, *IT* inferior turbinate

healthy adults have a septal deviation [8, 9]. Therefore, many septal deviations are asymptomatic. Our exclusion criterion was based on the current gold-standard measure of subjective perception of nasal obstruction, namely the NOSE score [14]. As described above, subjects with NOSE score > 32 were excluded. The cutoff value of 32 was based on the mean NOSE score plus one standard deviation of healthy subjects (i.e., 15 + 17 = 32) from a recent systematic literature review [17].

Benchmark healthy septum geometry

Creation of nasal airspace models

Cone-beam CT scans of the healthy subjects were obtained with 0.5 mm thickness and in-plane resolution of 0.5 mm. Conventional CT scans of the NAO patient were obtained pre-surgery and 5 months post-surgery with 0.6 mm thickness and in-plane resolution of 0.3 mm. The scans were imported into medical imaging software (Mimics 19.0; Materialise, Ann Arbor, MI) and 3D models of the nasal airspace were created using a threshold between − 1024 and − 300 Hounsfield units and manually removing the paranasal sinuses. All models were oriented with the Z-axis in the anterior–posterior direction, the Y-axis in the inferior–superior direction, and the X-axis in the lateral direction.

Geometry of healthy nasal septum

In the healthy cohort, septal geometries for all 47 subjects were reconstructed from the available airspace models [13]. To create the septal geometries from the airspace models, coronal and axial planes with 2 mm distance between neighboring planes were intersected with the left and right cavities to generate a point cloud representing the walls of the nasal cavities.

Septal thickness was defined as the horizontal distance between the two sides of the septum (Fig. 2b). Septal deviation was defined as the horizontal distance from the septum centerline to a straight reference line crossing the top and bottom of the septum on each coronal plane (Fig. 2c). A benchmark 3D healthy septum geometry was obtained by averaging the nasal septum geometry from the 47 healthy subjects. To account for interindividual variation in septum size, the nasal septum was normalized by its length and height. Septal length (l_{Septum}) was defined as the distance from the posterior end of the nostril to nasal choana (Fig. 3a). The normalized distance from nostrils (D) was defined as

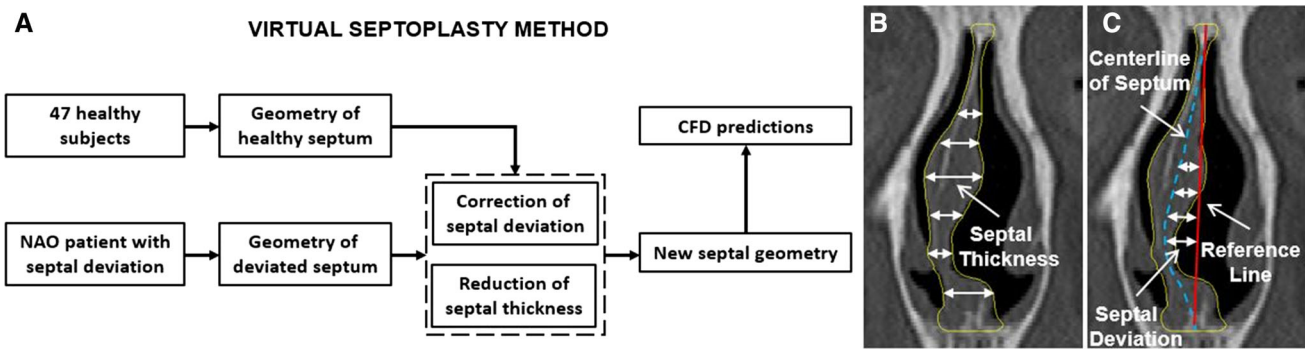

Fig. 2 Overview of the virtual septoplasty method. **a** The method is based on the correction of the septal deviation and reduction of septal thickness. **b** Septal thickness is measured horizontally from the nasal floor to the nasal roof in all coronal sections from nostrils to choana. **c** Septal deviation is defined as the distance from the septal centerline to the straight reference line that defines a straight septum

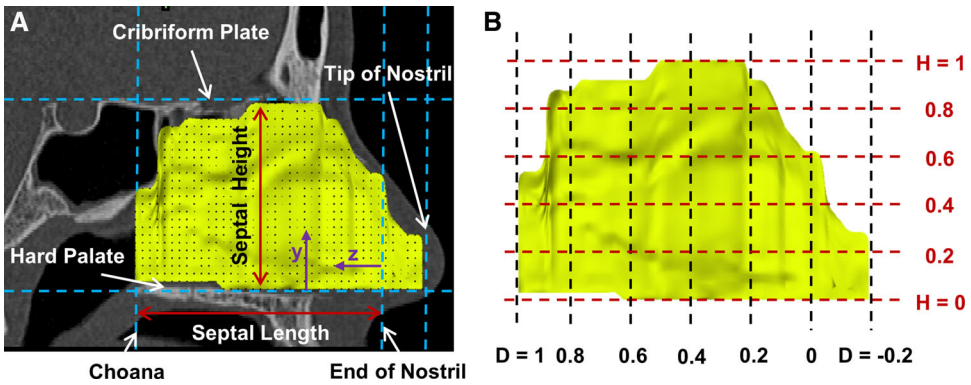

Fig. 3 Anatomical landmarks used to normalize the septal geometry among the 47 healthy subjects. **a** Septal geometry reconstructed from point cloud showing the definition of septal height and septal length. **b** Definition of the normalized distance from end of the nostrils (D) and the normalized distance from nasal floor (H)

$D = z/l_{\text{septum}}$, where z is the distance from the posterior end of the nostrils. Septal height (h_{septum}) was defined as the distance from the hard palate to the cribriform plate at coronal section $D = 0.5$ (Fig. 3a). The normalized height (H) was defined as $H = y/h_{\text{septum}}$, where y is the distance from the hard palate (Fig. 3b).

Geometry of NAO nasal septum

The geometry of the NAO septum was segmented in Mimics 19.0 and imported into ICEM-CFD 18.1 (ANSYS, Canonsburg, PA), where it was also intersected with a grid of coronal and axial planes to obtain a point cloud. Septal thickness and septal deviation were computed from the point cloud as explained above (Fig. 2b, c).

Virtual septoplasty method

The normalized healthy septum geometry was scaled to the dimensions of the NAO septum (by height and length) and coregistered with the NAO septum geometry. This allows point-by-point comparison (y and z coordinates) of septal deviation and thickness in the NAO septum versus the benchmark healthy septum geometry. Virtual septoplasty was implemented in MATLAB R2016a (MathWorks, Natick, MA) in two steps, namely (1) correction of septal deviation and (2) correction of septal thickness (Fig. 2). In step 1, points on the septum centerline whose deviation was greater than 2 mm were moved onto the reference line that defines zero deviation. (The 2 mm threshold was based on the fact that deviations exceeding 2 mm were rarely observed in the anterior nose in our healthy cohort—see "Results.") In step 2, septal thickness in the NAO patient was reduced to the benchmark septal thickness everywhere where septal thickness in the NAO patient exceeded the benchmark healthy septal thickness. After steps 1 and 2, smoothing was performed along the boundaries of the modified region to eliminate sudden jumps in the septal geometry.

The airspace virtual septoplasty model was created by importing the corrected 3D septum back into the medical imaging software (Mimics), where Boolean operations were performed to replace the pre-surgery septum with the corrected septum. Wherever the corrected septum touched the turbinates, a one-pixel layer of tissue from the septum was converted into air to reproduce the fact there is no overlap between the septum and turbinates after real surgical procedures.

Computational fluid dynamics simulations

Post-surgical changes in nasal aerodynamics were quantified via steady-state, laminar, inspiratory airflow simulations in ANSYS Fluent 18.1. The assumption of laminar flow for low breathing rates is supported by experiments [19, 20]. The governing equations are the Navier–Stokes and continuity equations for steady-state incompressible flow:

$$\mathbf{u}.\nabla\mathbf{u} = -\frac{1}{\rho}\nabla p + \nu\nabla^2\mathbf{u} \quad (1)$$

$$\nabla.\mathbf{u} = 0 \quad (2)$$

where $\mathbf{u}$ is the velocity vector, p is pressure, $\rho = 1.204$ kg m^{-3} is air density, and $\nu = 1.5 \times 10^{-5}$ m^2 s^{-1} is the kinematic viscosity of air.

Tetrahedral meshes were created in ANSYS ICEM-CFD 18.1 with approximately 4 million cells, which provides a good balance between accuracy and computational cost based on a previous mesh density study [21]. All tetrahedral elements had an aspect ratio above 0.3, thus avoiding highly distorted elements that could cause numerical errors. The CFD simulations were performed with the following boundary conditions: (1) inlet pressure at the nostrils equal to atmospheric pressure, (2) no slip at the walls, and (3) outlet pressure set to a constant negative value as required to obtain a bilateral flow rate of 250 ml s^{-1}, which represents an adult breathing at rest [22]. The outlet pressure required to reach a bilateral flow rate of 250 ml s^{-1} was determined by running preliminary simulations to quantify the relationship between outlet pressure and flow rate. Nasal resistance (R) was defined as the ratio of the total pressure drop (ΔP) from nostrils to outlet to the volume flow rate (Q)

$$R = \frac{\Delta P}{Q}$$

Airflow partitioning was defined as the ratio of unilateral flow to bilateral flow. Airspace cross-sectional areas from nostrils to choana were computed perpendicular to flow streamlines using the method described by Garcia and colleagues (2016) [23]. This method, dubbed 'computational streamline rhinometry', provides an area versus distance curve that is similar to acoustic rhinometry measurements [23].

CFD variables in the NAO patient are compared to normative ranges reported by Borojeni et al. [13]. The normative ranges, which were derived from the same 47 healthy subjects used to develop the benchmark healthy septum geometry in this study, were targeted to contain 95% of the healthy population and computed using a nonparametric method based on order statistics.

Results

Benchmark healthy septum geometry

The benchmark healthy septum geometry obtained from averaging the geometry of the nasal septa from 47 healthy subjects is shown in Fig. 4. Septal thickness is smallest in the olfactory cleft region ($H > 0.8$) and highest at the septal swell body (Fig. 4a) as can be easily visualized in coronal slices (Fig. 4d). The septal swell body is the bulge located anteriorly ($D = 0.1$–0.4) about halfway between the nasal floor and the nasal roof ($H = 0.3$–0.8). The benchmark healthy septum geometry is symmetric by design, that is, its septal deviation is zero everywhere. However, many subjects in our healthy cohort had septal deviations, which were often located in the posterior nose (Fig. 4b) and whose magnitude was relatively small compared to septal thickness (Fig. 4e). The data displayed in Fig. 4b, e represent the greatest degree of septal deviation at each location (i.e., D, H coordinates) among the 47 healthy subjects. Since most patients who undergo septoplasty have anterior septal deviations [10], and anterior septal deviations were rarely greater than 2 mm in our healthy cohort (Fig. 4b), we defined a threshold septal deviation of 2 mm as the criterion to identify the region of abnormal geometry requiring surgical correction.

Virtual septoplasty

The patient with NAO had an anterior septal deviation toward the right cavity (Fig. 1a). Analysis of the three-dimensional septal geometry revealed that the deviation exceeded 6 mm (Fig. 5c). To clearly identify regions of abnormal septal geometry, the benchmark healthy septum was rescaled using the septal length ($l_{\text{Septum}} = 66$ mm) and septal height ($h_{\text{Septum}} = 46$ mm) of the NAO patient, so that a point-by-point comparison could be performed between the NAO septum and the benchmark geometry. This point-by-point comparison revealed the precise location of hotspots of septal thickness and septal deviation (Fig. 5d, e). Virtual septoplasty was performed by correcting septal deviation and septal thickness. As described in "Materials and methods," septal deviation was corrected where it exceeded 2 mm, while septal thickness was reduced where it exceeded the thickness in the benchmark geometry. After virtual septoplasty, the nasal septum was straight, while retaining its three-dimensional shape (Figs. 5f–h, 6a).

Predicted versus actual changes in nasal geometry

Calculation of airspace cross-sectional areas (CSA) demonstrated a severe constriction in the anterior right cavity of the NAO patient as compared to the range observed in healthy subjects (Fig. 7). The NAO patient had CSA that

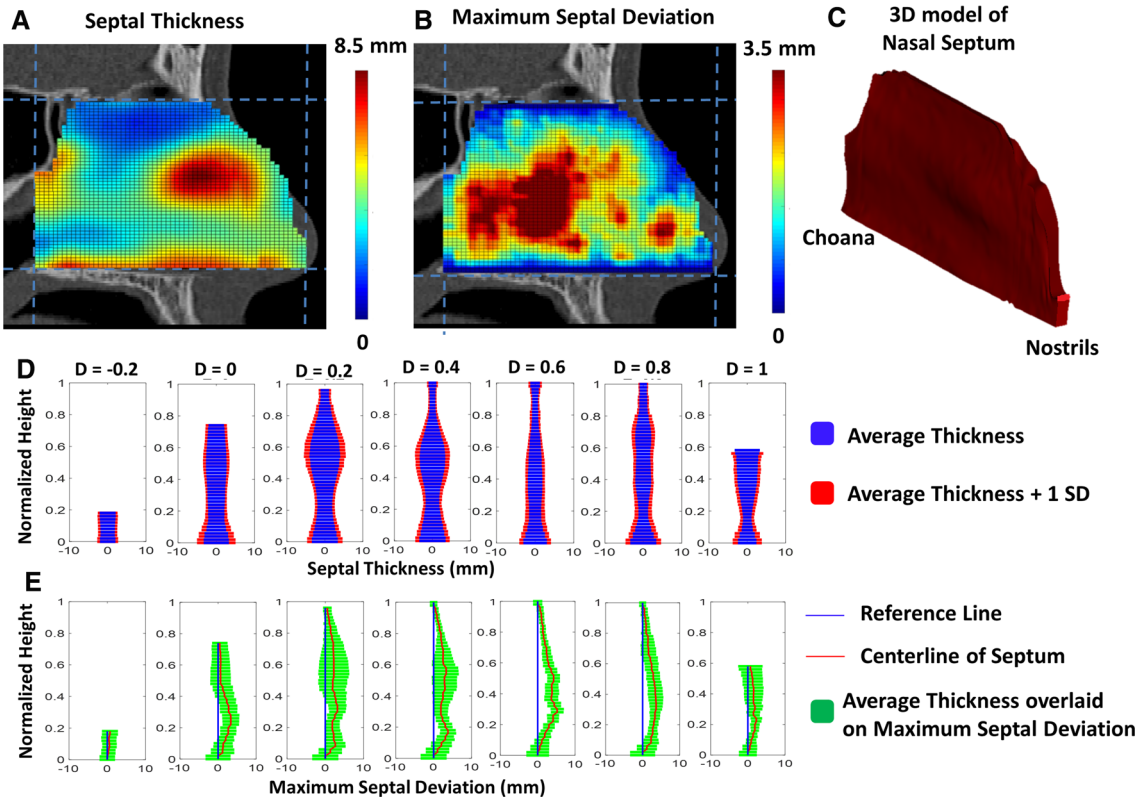

Fig. 4 Benchmark healthy septum geometry and maximum range of septal deviation observed in 47 healthy subjects. **a** Colormap of septal thickness in the benchmark healthy septum geometry representing the average septal thickness in 47 healthy subjects. **b** Colormap of maximum septal deviation representing the highest degree of deviation observed in the healthy subjects. **c** Benchmark healthy septum geometry based on average dimensions. **d** Average septal thickness versus height from nasal floor for seven equally spaced coronal planes from nostrils ($D = -0.2$) to nasal choana ($D = 1$). **e** Maximum septal deviation among the 47 healthy subjects versus height from nasal floor for the same coronal planes

exceeded or were within the healthy range in the left cavity. After virtual septoplasty, a more uniform distribution of CSA was predicted between the left and right cavities with CSA falling mostly within the healthy range in both cavities. These predicted geometrical changes were compared to actual anatomical changes observed in the post-surgery CT scan, which represented the outcome of a standard septoplasty that was not informed by the virtual model (Figs. 6b, 7). The virtual septoplasty model turned out to be a slight overcorrection of the septum as compared to the post-surgery CT scan (Fig. 6b); thus, it overestimated the increase in CSA in the right cavity (Fig. 7c). The post-surgery CT scan showed gains in cross-sectional area in both the left and right cavities as compared to pre-surgery (Fig. 7), but these changes were due in part to changes in mucosal engorgement related to the nasal cycle between the pre-surgery and post-surgery CT scans (Fig. 6). Nasal cycling was not incorporated in the virtual septoplasty model.

Predicted versus actual changes in nasal airflow

Pre-surgery bilateral nasal resistance in the NAO patient was 0.06 Pa s ml^{-1}, which was within the normative range of 0.017–0.12 Pa s ml^{-1} derived from the 47 healthy subjects [13]. The severe constriction in the anterior right cavity resulted in a minimal cross-sectional area (mCSA = 0.05 cm^2) that was outside the normative range (0.24–1.21 cm^2). This severe constriction was associated with a high unilateral resistance in the right cavity (R = 0.91 Pa s ml^{-1}) that was outside the normative range for unilateral resistances (0.029–0.32 Pa s ml^{-1}). The unequal resistances of the left and right cavities led to an unbalanced airflow partitioning pre-surgery with only 11% of air flowing through the right nostril, which was also outside the normative range for airflow partitioning (23.8–76.2%). Altogether, these abnormalities in nasal airflow support the surgeon's decision to perform septoplasty in this patient.

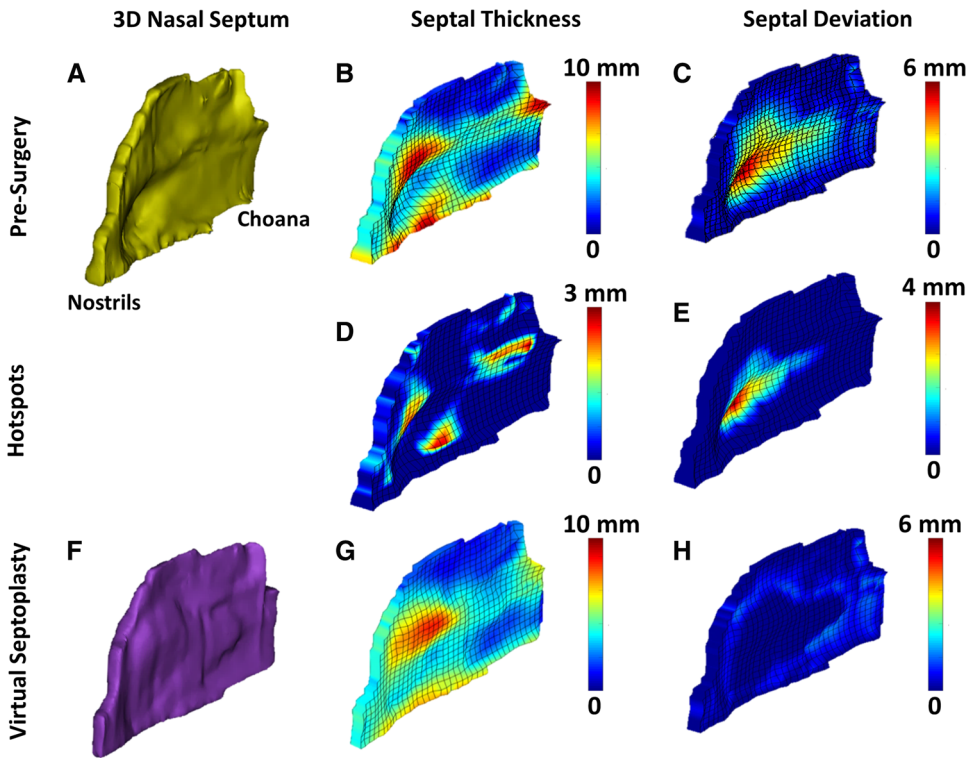

Fig. 5 Virtual septoplasty method applied to one NAO patient with a deviated septum. **a** 3D geometry of nasal septum pre-surgery. **b** Colormap of septal thickness pre-surgery. **c** Colormap of septal deviation pre-surgery. **d**, **e** Difference between septal anatomy in the NAO patient versus the average dimensions of a healthy nasal septum. The colormaps highlight the regions where septal thickness exceeds the average thickness observed in the healthy cohort and where septal deviation exceeds the 2 mm threshold. **f** 3D geometry of nasal septum after virtual septoplasty. **g**, **h** Septal thickness and septal deviation after virtual septoplasty

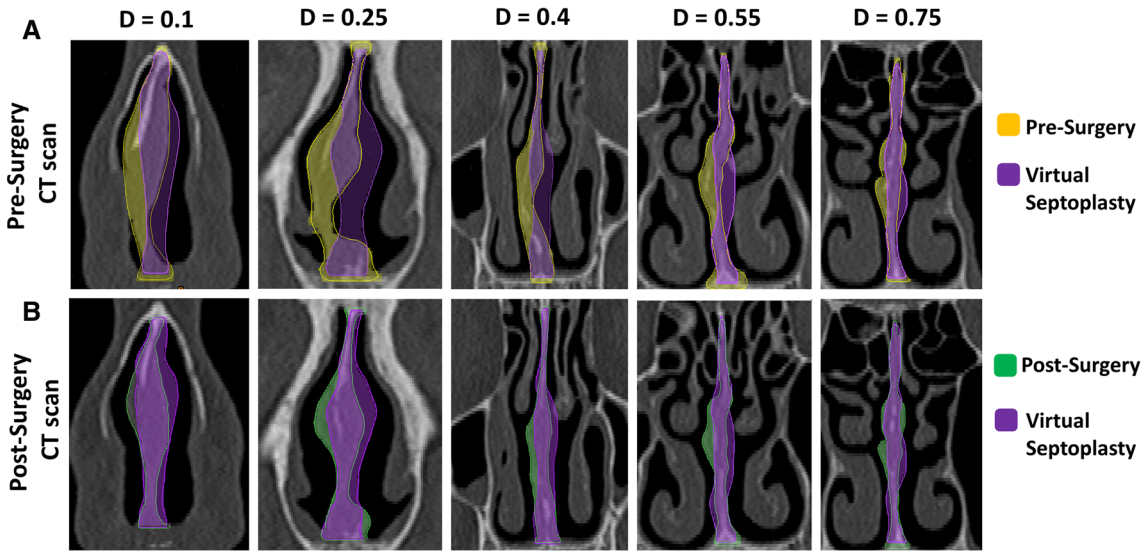

Fig. 6 Nasal septal geometry in the virtual septoplasty model compared with **a** pre-surgery CT scan and **b** post-surgery CT scan. The virtual septoplasty model was based on the pre-surgery CT scan using the systematic algorithm without knowledge of the post-surgery CT scan

Virtual septoplasty predicted that the percentage of air flowing through the right nostril would increase from 11 to 42%, which was in good agreement with the 36% observed in the actual post-surgery model (Fig. 8a). More symmetric airflow partitioning between the left and right nostrils was due to more even unilateral resistances in the left and right cavities in the virtual surgery model (0.06 vs. 0.08 Pa s ml^{-1}) and post-surgery model (0.05 vs. 0.08 Pa s ml^{-1}) as compared to the pre-surgery model (0.07 vs. 0.91 Pa s ml^{-1}) (Fig. 8b). The sharp reduction in right side resistance is largely due to the increase in minimal cross-sectional area from 0.05 cm^2 pre-surgery to 0.54 cm^2 in the virtual septoplasty model and 0.50 cm^2 in the post-surgery model (Fig. 7). Bilateral resistance was predicted to decrease from 0.06 Pa s ml^{-1} pre-surgery to 0.03 Pa s ml^{-1} in both the virtual septoplasty and post-surgery models (Fig. 8b).

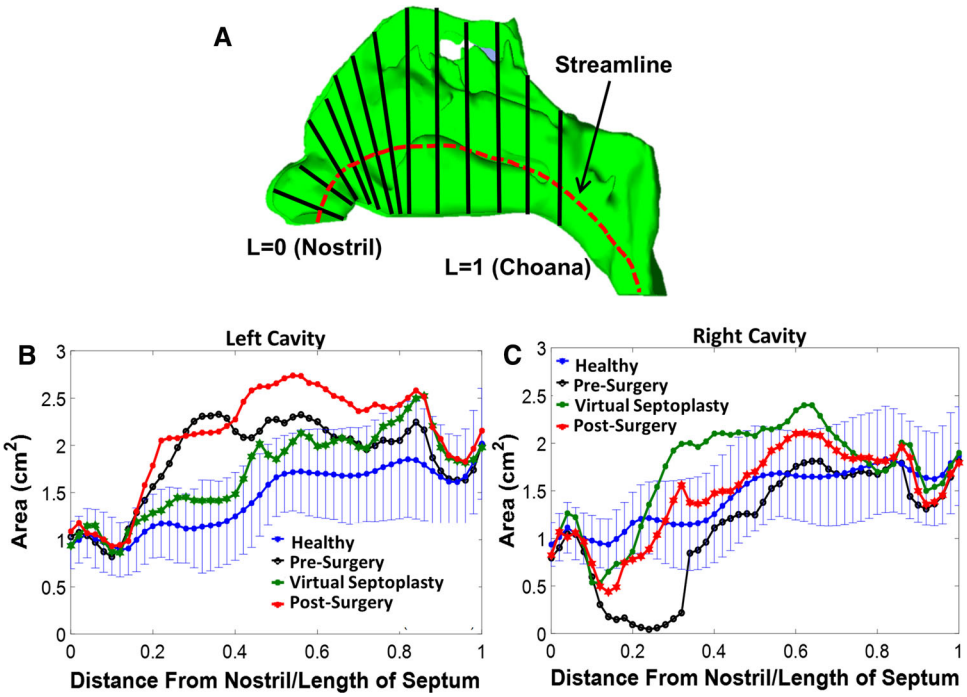

Fig. 7 Airspace cross-sectional areas. **a** Airspace cross-sectional areas were measured perpendicular to airflow streamlines in the anterior nose and perpendicular to the nasal floor in the posterior nose (L represents the normalized distance along the streamline). **b**, **c** Airspace cross-sectional areas versus the normalized distance from nostrils in the pre-surgery, virtual septoplasty, and post-surgery models compared to the average (± 1 standard deviation) among 47 healthy subjects

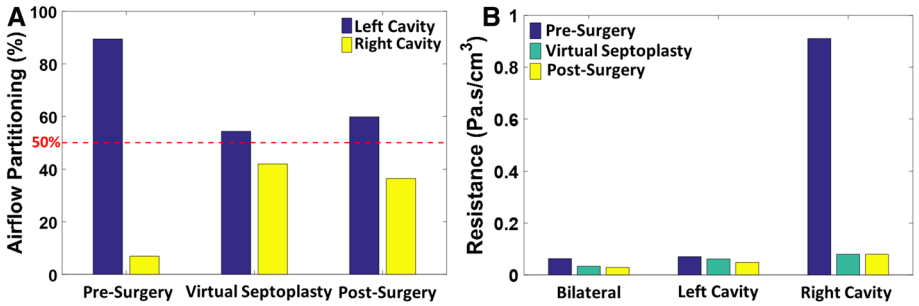

Fig. 8 CFD results. **a** Airflow partitioning between left nostril and right nostril in the pre-surgery, virtual septoplasty, and post-surgery models. **b** Bilateral and unilateral resistances in the pre-surgery, virtual septoplasty, and post-surgery models

Discussion

Septoplasty is the most common nasal surgical procedure performed in adults [24]. Yet, objective criteria to select patients for surgery are lacking and its effectiveness remains uncertain [5]. In 2015, the American Academy of Otolaryngology had to rely on expert opinion to promote evidence-based care for patients with nasal obstruction associated with a septal deviation [25]. The panel of experts agreed that septoplasty is "a surgical procedure designed to correct a deviated nasal septum for the purpose of improving nasal function, form, or both." However, the panel did not reach a consensus on the statement that "acoustic rhinometry and rhinomanometry can be helpful for patients who present with nasal obstruction as a primary complaint." In other words, otolaryngologists agree that the goal of septoplasty is to improve nasal function, but there is no consensus on which objective method to use to quantify nasal function and to inform surgical decisions.

A recent systematic literature review concluded that the current body of evidence does not support firm conclusions on the effectiveness of septoplasty [26]. Although most studies included in the review reported significant improvement in objective outcomes after septoplasty, the authors highlighted the methodological flaws of these studies and concluded that the risk of bias was high. This knowledge gap motivated the first randomized controlled clinical trial of septoplasty versus non-surgical management of nasal obstruction in adults with a deviated septum [27]. This clinical trial found that patients undergoing septoplasty had greater improvement in subjective nasal patency and quality of life scores than patients in the non-surgical group. Objective measurements of peak nasal inspiratory airflow (PNIF) demonstrated higher airflow in the septoplasty group. However, nasal resistance measured with rhinomanometry did not show a statistically significant difference between the septoplasty and non-surgical groups. The authors attributed the inconsistency between the two objective measures to the poor responsiveness of rhinomanometry [27, 28]. One shortcom-

ing of this clinical trial is that it did not include sham surgery, thus it did not account for the placebo effect in the surgical group. Also, although rhinomanometry is prone to large errors [29], its responsiveness is sufficient to document the reduction in nasal resistance after mucosal decongestion with nasal sprays [30]. This suggests that the effect size of septoplasty is smaller than the uncertainty of rhinomanometric measurements. Therefore, there is a need for more accurate objective measures of nasal obstruction to inform surgical decisions and improve the success rate of NAO surgery.

There is hope that virtual surgery planning based on CFD simulations may fill this clinical need for objective measures of nasal airflow. Virtual surgery planning software is currently available [2, 31], but several challenges must be overcome before this technology can be adopted in clinical practice. One major challenge that the current study aims to address is that existing virtual surgery methods are based on manual editing of nasal anatomy models [18, 32]. Manual editing is performed frame-by-frame in two-dimensional CT images [18, 33] or by removing tissue layers in three-dimensional models [31]. These manual editing techniques are subjective and labor-intensive since it can take several hours of work to create a virtual surgery model. This is a significant barrier to the adoption of this technology in clinical care, since it makes the technology expensive and impractical. One major contribution of this manuscript is the proposal of a systematic, algorithmic method for virtual septoplasty that has the potential to be fully automated. Although future virtual surgery environments will likely include the ability for user-interaction so that surgeons may alter the geometry by hand if they disagree with the algorithm's proposed anatomical changes, automated methods are expected to speed up the surgical planning, reduce costs, and thus facilitate adoption of this technology in clinical care.

Another key contribution of this work is the development of the first benchmark geometry of a healthy nasal septum, which was based on the average dimensions of the nasal septa from 47 healthy individuals (Fig. 4). The importance of the benchmark geometry is that it allows identification of regions of abnormal septal anatomy through a point-by-point comparison between the septal geometry of a patient with NAO and the benchmark geometry (Fig. 5d, e). Classification systems have been previously reported to quantify the severity of septal deviation, but these classification systems were based on visual inspection of septal anatomy via rhinoscopy and endoscopy [34]. Our computational method, which is based on measurements of septal thickness and septal deviation on CT scans (Fig. 2b, c), provides a new classification system that is both quantitative and objective. Importantly, posterior septal deviations that deviate as much as 3.5 mm from the midline were observed in our healthy cohort, but the anterior septum was mostly straight in the 47 healthy subjects (Fig. 4b). These observations are consistent with previous reports that anterior septal deviations are more likely to be clinically relevant because they increase nasal resistance more than posterior deviations [10].

Some limitations of this work must be acknowledged. First, our 3D models of the nasal airspace were obtained via manual segmentation from CT scans. Segmentation is currently the most labor-intensive step in the CFD analysis, which limits the sample size in CFD studies of nasal airflow. Automatic segmentation of the nasal anatomy with techniques such as machine learning is expected to overcome this limitation in the near future. Second, another limitation of our virtual septoplasty method is that we did not account for fluctuations in mucosal engorgement associated with the nasal cycle. Fluctuations in mucosal engorgement lead to significant oscillations in unilateral nasal resistance and airflow partitioning [35]. Virtual correction of CT scans showing extreme nasal cycling has been shown to increase the correlation between CFD variables and subjective nasal patency scores, and thus, it should be considered when implementing virtual surgery planning in clinical care [36, 37]. Third, another limitation of this work is that the virtual septoplasty method was illustrated in a single patient with NAO. Given the substantial anatomical variability among patients, additional studies are needed to demonstrate the utility of the virtual septoplasty method in a larger sample of patients. Fourth, this was a retrospective study. Good agreement was found between anatomical and airflow changes predicted by our virtual septoplasty method and observed post-surgery. However, prospective studies are needed to test the hypothesis that virtual surgery planning will increase patient satisfaction and improve objective outcomes after septoplasty. Finally, NAO patients often undergo septoplasty in combination with other surgical procedures, such as inferior turbinate reduction and functional rhinoplasty. Therefore, our virtual septoplasty method will be most useful when implemented in a virtual surgery environment that also includes automated methods for planning inferior turbinate reduction, functional rhinoplasty, and other nasal surgery procedures.

In summary, there is no consensus among physicians on quantitative criteria to select patients for septoplasty. Surgical planning is currently based on subjective symptoms and surgeon judgment, which lead to a substantial fraction of patients reporting persistent symptoms postoperatively. This manuscript reports the first systematic virtual surgery method to identify patients with septal anatomy outside the normal range and to predict post-surgical changes in nasal airflow. The method was applied to one NAO patient and showed good agreement with actual surgical outcomes. Future implementation of this method in automated virtual surgery planning software has the potential to improve septoplasty outcomes.

Funding This study was funded by Grant R01EB009557 from the National Institutes of Health/National Institute of Biomedical Imaging and Bioengineering to the Medical College of Wisconsin (MCW) and by subcontract from MCW to the University of North Carolina at Chapel Hill and Duke University.

Compliance with ethical standards

Conflict of interest The authors declare that they have no conflict of interest.

Ethical approval All procedures were performed in accordance with the ethical standards of the institutional review boards at The Medical College of Wisconsin and Marquette University and of the 1964 Helsinki Declaration and its later amendments.

Informed consent Informed consent was obtained from all individual participants included in the study.

References

1. Hildebrandt T, Bruning JJ, Lamecker H, Zachow S, Heppt WJ, Schmidt N, Goubergrits L (2019) Digital analysis of nasal airflow facilitating decision support in rhinosurgery. Facial Plast Surg 35(1):3–8. https://doi.org/10.1055/s-0039-1677720
2. Quammen CW, Taylor RM 2nd, Krajcevski P, Mitran S, Enquobahrie A, Superfine R, Davis B, Davis S, Zdanski C (2016) The virtual pediatric airways workbench. Stud Health Technol Inform 220:295–300
3. Vanhille DL, Garcia GJM, Asan O, Borojeni AAT, Frank-Ito DO, Kimbell JS, Pawar SS, Rhee JS (2018) Virtual surgery for the nasal airway: a preliminary report on decision support and technology acceptance. JAMA Facial Plast Surg 20(1):63–69. https://doi.org/10.1001/jamafacial.2017.1554
4. Sanmiguel-Rojas E, Burgos MA, Esteban-Ortega F (2018) Nasal surgery handled by CFD tools. Int J Numer Methods Biomed Eng. https://doi.org/10.1002/cnm.3126
5. Roblin DG, Eccles R (2002) What, if any, is the value of septal surgery? Clin Otolaryngol Allied Sci 27(2):77–80
6. Sundh C, Sunnergren O (2015) Long-term symptom relief after septoplasty. Eur Arch Oto-Rhino-Laryngol 272(10):2871–2875. https://doi.org/10.1007/s00405-014-3406-7
7. Bhattacharyya N (2010) Ambulatory sinus and nasal surgery in the United States: demographics and perioperative outcomes. Laryngoscope 120(3):635–638. https://doi.org/10.1002/lary.20777
8. Jones NS, Strobl A, Holland I (1997) A study of the CT findings in 100 patients with rhinosinusitis and 100 controls. Clin Otolaryngol Allied Sci 22(1):47–51
9. Min YG, Jung HW, Kim CS (1995) Prevalence study of nasal septal deformities in Korea: results of a nation-wide survey. Rhinology 33(2):61–65
10. Garcia GJ, Rhee JS, Senior BA, Kimbell JS (2010) Septal deviation and nasal resistance: an investigation using virtual surgery and computational fluid dynamics. Am J Rhinol Allergy 24(1):e46-53. https://doi.org/10.2500/ajra.2010.24.3428
11. Holmstrom M (2010) The use of objective measures in selecting patients for septal surgery. Rhinology 48(4):387–393. https://doi.org/10.4193/Rhino10.072
12. Andre RF, Vuyk HD, Ahmed A, Graamans K, Nolst Trenite GJ (2009) Correlation between subjective and objective evaluation of the nasal airway. A systematic review of the highest level of evidence. Clin Otolaryngol 34(6):518–525. https://doi.org/10.1111/j.1749-4486.2009.02042.x
13. Borojeni AAT, Garcia GJM, Moghaddam MG, Frank-Ito DO, Kimbell JS, Laud PW, Koenig LJ, Rhee JS (2020) Normative ranges of nasal airflow variables in healthy adults. Int J Comput Assist Radiol Surg 15(1):87–98. https://doi.org/10.1007/s11548-019-02023-y
14. Stewart MG, Witsell DL, Smith TL, Weaver EM, Yueh B, Hannley MT (2004) Development and validation of the nasal obstruction symptom evaluation (NOSE) scale. Otolaryngol Head Neck Surg 130(2):157–163. https://doi.org/10.1016/j.otohns.2003.09.016
15. Kimbell JS, Frank DO, Laud P, Garcia GJ, Rhee JS (2013) Changes in nasal airflow and heat transfer correlate with symptom improvement after surgery for nasal obstruction. J Biomech 46(15):2634–2643. https://doi.org/10.1016/j.jbiomech.2013.08.007
16. Sullivan CD, Garcia GJ, Frank-Ito DO, Kimbell JS, Rhee JS (2014) Perception of better nasal patency correlates with increased mucosal cooling after surgery for nasal obstruction. Otolaryngol Head Neck Surg 150(1):139–147. https://doi.org/10.1177/0194599813509776
17. Rhee JS, Sullivan CD, Frank DO, Kimbell JS, Garcia GJ (2014) A systematic review of patient-reported nasal obstruction scores: defining normative and symptomatic ranges in surgical patients. JAMA Facial Plast Surg 16(3):219–225. https://doi.org/10.1001/jamafacial.2013.2473 **(quiz 232)**
18. Frank-Ito DO, Kimbell JS, Laud P, Garcia GJM, Rhee JS (2014) Predicting postsurgery nasal physiology with computational modeling: current challenges and limitations. Otolaryngol Head Neck Surg 151(5):751–759. https://doi.org/10.1177/0194599814547497
19. Kelly JT, Prasad AK, Wexler AS (2000) Detailed flow patterns in the nasal cavity. J Appl Physiol 89(1):323–337. https://doi.org/10.1152/jappl.2000.89.1.323
20. Li C, Jiang J, Dong H, Zhao K (2017) Computational modeling and validation of human nasal airflow under various breathing conditions. J Biomech 64:59–68. https://doi.org/10.1016/j.jbiomech.2017.08.031
21. Frank-Ito DO, Wofford M, Schroeter JD, Kimbell JS (2016) Influence of mesh density on airflow and particle deposition in sinonasal airway modeling. J Aerosol Med Pulm Drug Deliv 29(1):46–56. https://doi.org/10.1089/jamp.2014.1188
22. Garcia GJ, Schroeter JD, Segal RA, Stanek J, Foureman GL, Kimbell JS (2009) Dosimetry of nasal uptake of water-soluble and reactive gases: a first study of interhuman variability. Inhal Toxicol 21(7):607–618. https://doi.org/10.1080/08958370802320186
23. Garcia GJM, Hariri BM, Patel RG, Rhee JS (2016) The relationship between nasal resistance to airflow and the airspace minimal cross-sectional area. J Biomech 49(9):1670–1678. https://doi.org/10.1016/j.jbiomech.2016.03.051
24. Manoukian PD, Wyatt JR, Leopold DA, Bass EB (1997) Recent trends in utilization of procedures in otolaryngology-head and neck surgery. Laryngoscope 107(4):472–477
25. Han JK, Stringer SP, Rosenfeld RM, Archer SM, Baker DP, Brown SM, Edelstein DR, Gray ST, Lian TS, Ross EJ, Seiden AM, Setzen M, Tollefson TT, Ward PD, Welch KC, Wise SK, Nnacheta LC (2015) Clinical consensus statement: septoplasty with or without inferior turbinate reduction. Otolaryngol Head Neck Surg 153(5):708–720. https://doi.org/10.1177/0194599815606435
26. van Egmond M, Rovers MM, Tillema AHJ, van Neerbeek N (2018) Septoplasty for nasal obstruction due to a deviated nasal septum in adults: a systematic review. Rhinology 56(3):195–208. https://doi.org/10.4193/Rhin18.016
27. van Egmond M, Rovers MM, Hannink G, Hendriks CTM, van Heerbeek N (2019) Septoplasty with or without concurrent turbinate surgery versus non-surgical management for nasal obstruction in adults with a deviated septum: a pragmatic, ran-

domised controlled trial. Lancet 394(10195):314–321. https://doi.org/10.1016/S0140-6736(19)30354-X
28. van Egmond M, van Heerbeek N, Ter Haar ELM, Rovers MM (2017) Clinimetric properties of the Glasgow health status inventory, Glasgow benefit inventory, peak nasal inspiratory flow, and 4-phase rhinomanometry in adults with nasal obstruction. Rhinology 55(2):126–134. https://doi.org/10.4193/Rhin16.296
29. Carney AS, Bateman ND, Jones NS (2000) Reliable and reproducible anterior active rhinomanometry for the assessment of unilateral nasal resistance. Clin Otolaryngol Allied Sci 25(6):499–503
30. Clarke RW, Cook JA, Jones AS (1995) The effect of nasal mucosal vasoconstriction on nasal airflow sensation. Clin Otolaryngol Allied Sci 20(1):72–73
31. Burgos MA, Sanmiguel-Rojas E, Singh N, Esteban-Ortega F (2018) DigBody((R)): a new 3D modeling tool for nasal virtual surgery. Comput Biol Med 98:118–125. https://doi.org/10.1016/j.compbiomed.2018.05.016
32. Hemtiwakorn K, Mahasitthiwat V, Tungjitkusolmun S, Hamamoto K, Pintavirooj C (2015) Patient-specific aided surgery approach of deviated nasal septum using computational fluid dynamics. IEEJ Trans Electr Electron Eng 10(3):274–286. https://doi.org/10.1002/tee.22084
33. Frank-Ito DO, Kimbell JS, Borojeni AAT, Garcia GJM, Rhee JS (2019) A hierarchical stepwise approach to evaluate nasal patency after virtual surgery for nasal airway obstruction. Clin Biomech (Bristol, Avon) 61:172–180. https://doi.org/10.1016/j.clinbiomech.2018.12.014
34. Gu JT, Kaplan S, Greenfield S, Calloway H, Wong BJF (2019) Validation of a septoplasty deformity grading system for the evaluation of nasal obstruction. Laryngoscope 129(3):586–593. https://doi.org/10.1002/lary.27365
35. Flanagan P, Eccles R (1997) Spontaneous changes of unilateral nasal airflow in man. A re-examination of the 'nasal cycle'. Acta Oto-Laryngol 117(4):590–595. https://doi.org/10.3109/00016489709113443
36. Gaberino C, Rhee JS, Garcia GJ (2017) Estimates of nasal airflow at the nasal cycle mid-point improve the correlation between objective and subjective measures of nasal patency. Respir Physiol Neurobiol 238:23–32. https://doi.org/10.1016/j.resp.2017.01.004
37. Patel RG, Garcia GJ, Frank-Ito DO, Kimbell JS, Rhee JS (2015) Simulating the nasal cycle with computational fluid dynamics. Otolaryngol Head Neck Surg 152(2):353–360. https://doi.org/10.1177/0194599814559385